Japanese Journal of Applied Physics
Vol. 43, No. 12, 2004, pp. 0000–0000

Orientation Distribution and Fiber Texture of Highly Oriented Piezoceramics: $(1-x)PbMg_{1/3}Nb_{2/3}O_3$–$xPbTiO_3$ System

Mai Pham THI*, Henri HEMERY, Olivier DURAND and Hichem DAMMAK[1]

THALES Research & Technology France, 91404 Orsay Cedex, France
[1]*Laboratoire SPMS, UMR 8580 CNRS, École Centrale Paris, 92295 Châtenay-Malabry, France*

(Received June 8, 2004; revised August 9, 2004; accepted August 11, 2004; published xxxx yy, zzzz)

Textured $(1-x)PbMg_{1/3}Nb_{2/3}$–$xPbTiO_3$, (PMN–xPT), ceramics were synthesised by the homo template grain growth (HTGG) technique using PMN–PT nanoparticles and cubic single crystals seeds (templates). The orientation of the templates was obtained during tape casting. Sintering was performed under controlled O_2/PbO partial pressure. The fraction of textured ceramics was estimated by the Lotgering method at RT and above Tc. Textured tape cast ceramics display a quasi complete (001) texture ($f = 0.99$) in the cubic phase. The (011) pole figure reveals a (001) fibre texture in accordance with the optical observation. The texture was obtained in all volumes of ceramics and only a small orientation distribution was observed ($<6°$). [DOI: 10.1143/JJAP.43.dummy]

KEYWORDS: PMN–PT, textured ceramic, template grain growth, X-ray diffration

1. Introduction

Relaxor single crystals[1–4] based on compounds such as $Pb[(Zn_{1/3}Nb_{2/3})_{0.91}Ti_{0.09}]O_3$ (PZN–9%PT) and $Pb[(Mg_{1/3}Nb_{2/3})_{0.68}Ti_{0.32}]O_3$ (PMN–32%PT) have been attracting considerable attention, because of the large electromechanical coupling factor of the k_{33} mode of over 92% and the exceptional piezoelectric constant ($d_{33} = 2000\,pC/N$). These properties are related to the ability of a single crystal to be easily oriented along the non polar ⟨001⟩ direction during poling so that the maximum response can be obtained. In addition, the phase diagrams of PZN–PT and PMN–PT show the existence of monoclinic phases near the morphotropic phase boundary of 7–9%[5–7] and 29–37%,[8] respectively.

Orientation-dependent properties of single crystals lead to the prediction that ceramics exhibiting high degrees of appropriate crystallographic texture should have electromechanical properties approaching those of ⟨001⟩ oriented single crystals. Textured $Pb(Mg_{1/3}Nb_{2/3})O_3$–$PbTiO_3$ ceramics were obtained by the reactive template grain growth (RTGG) technique using $BaTiO_3$[9,10] or $SrTiO_3$ seeds.[11] Recently, we demonstrated that ceramics with a high ⟨001⟩ orientation were successfully obtained[12] by the homo template grain growth (HTGG) technique for PMN–PT ceramics with PMN–PT cubic template seeds.

The objectives of this study are to investigate the X-ray diffraction of textured PMN–35%PT ceramics obtained by the HTGG technique, as a function of temperature. θ–2θ spectra were recorded to estimate the fraction of textured ceramics. Omega scan and pole figures were recorded on textured ceramics in order to determine the degree of ⟨001⟩ alignment.

2. Experimental Methods

PMN–35%PT powders and few percent of PMN–25%PT cubic templates were mixed with an organic binder to obtain homogenous slurry. The mixture was tape cast using a doctor blade. Green tapes of 100–150 μm were dried, laminated and cut into samples of about 0.5 to 3 mm. Green tape cast ceramics (GTCC) were sintered under O_2 flow between 1150 and 1200°C for different durations.

A microstructure was recorded on as-sintered and polished surfaces using an optical microscope. Preliminary θ–2θ X-ray characterisations and pole figures were obtained at room temperature using, respectively, a Seifert MZ-IV goniometer in the Bragg–Brentano geometry and a Seifert MZ-IV four-circle goniometer, both equipped with a black curved graphite monochromator that selects the Cu-K_α wavelength. An advanced study of the texture is obtained using a high accuracy two-axis diffractometer with Cu-K_α monochromatic radiation issued from a Rigaku rotating anode (RU 300, 18 kW);[13] ceramics were fixed on a sample and mounted upon a HUBER goniometric head. A N_2 flow device was used to record spectra at 473 K in the cubic phase.

The texture fraction of the {001} planes was estimated from the XRD patterns using the Lotgering method. The Lotgering factor f is defined as the fraction of the area textured with the crystallographic plane of interest[14] using

$$f_{00l} = (P_{00l} - P_0)/(1 - P_0),$$

where $P_{00l} = \sum I_{00l} / \sum I_{hkl}$ and $P_0 = \sum I^0_{00l} / \sum I^0_{hkl}$, with I_{hkl} and I^0_{hkl} being the intensities of (hkl) peaks for the textured and randomly oriented sample, respectively. It is important to note that the analysed surface is about $\sim 1\,cm^2$ and the penetration depth of X-rays at 20–40 keV is a few microns. Furthermore, textured ceramics exhibit grains of about 50–200 μm size.

3. Results and Discussion

3.1 Texture fraction and Lotgering factor

XRD spectra recorded on the as-sintered ceramic surface are the same as those of green tape cast ceramics [Fig. 1(a)]. This shows that the ceramic sintered at 1100°C presents a spectrum relative to the random orientation ceramic in which a (110) peak of the highest intensity is observed [Fig. 1(b)]. For the sample sintered at 1150°C, a strong increase in (00l) diffraction peaks intensities was observed [Fig. 1(c)]. This intensity change indicates an increase in the crystallographic (00l) orientation of the tape cast textured ceramics (TCTC) samples. When ceramics were sintered at 1200°C for 10 h, the XRD spectrum presents only the peaks due to the (00l) orientation [Fig. 1(d)].

*E-mail address: mai.phamthi@thalesgroup.com

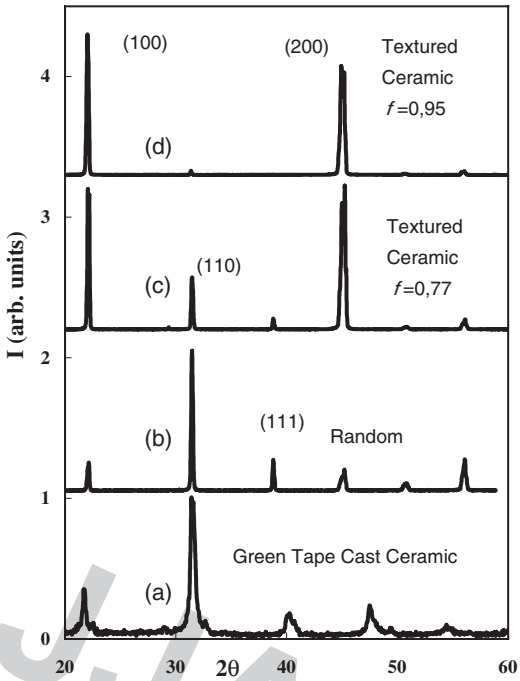

Fig. 1. X-ray diffraction spectra of green tape cast ceramics (a) and PMN–PT tape cast textured ceramics sintered at (b) 1100°C, (c) 1150°C and (d) 1200°C.

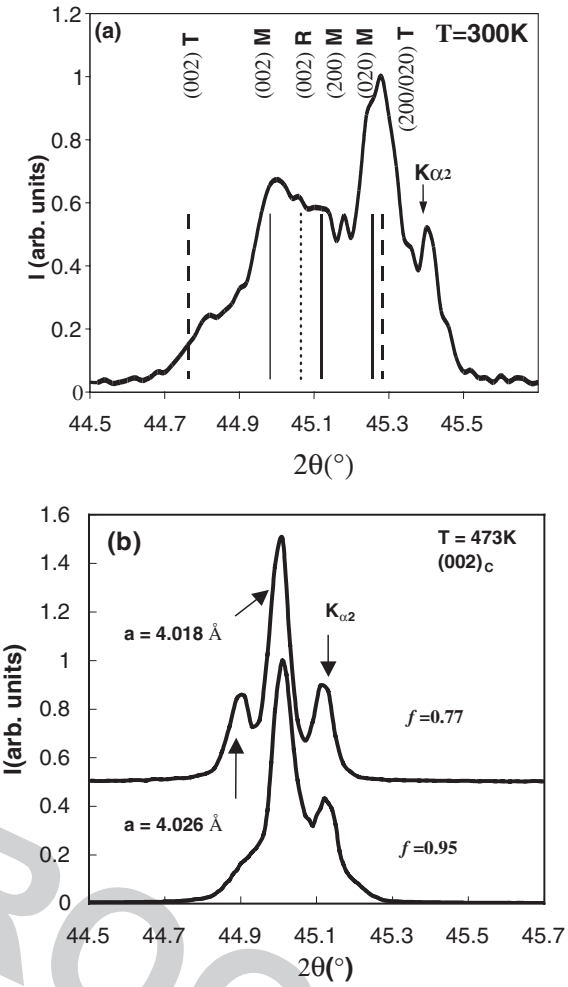

Fig. 2. X-ray diffraction spectra of {002} peak of sample displaying the Lotgering factor of 0.77 (a) at RT and (b) at 473 K in cubic phase of samples displaying the Lotgering factor of 0.77 and 0.95. At RT, PMN–34%PT and PMN–26%PT peaks are indicated which are respectively tetragonal, monoclinic and rhombohedral as defined by Singh and Pandey.[8)]

The texture fraction or Lotgering factor of textured samples was estimated from the XRD spectrum recorded at RT using all peaks up to the (222) reflection, i.e., 2θ up to 85°. For ceramics sintered at 1200°C and 1150°C for 10 h, the TCTC disks ($\Phi \sim 14$ mm) exhibit texture fractions of ~0.95 (sample A) and ~0.77 (sample B), respectively. These results seem to indicate that the texture development starts at around 1150°C and increases at a higher temperature and longer sintering duration.

At room temperature, the XRD spectra of the {002} reflection show a complex structure [Fig. 2(a)]. A doublet observed for the {002} reflection is generally attributed to the tetragonal symmetry. The more complex {002} peak profile observed for TCTC is probably due to the coexistence of the tetragonal and monoclinic phases for compositions in the range of the morphotropic phase boundary.[8)] In fact, Fig. 2 shows that at 300 K, a peak near 45.3° and a very broad band near 45° were observed. This could be due to the presence of a textured ceramic matrix (PMN–35%PT) in both monoclinic and tetragonal phases and cubic seeds in the rhombohedral phase (PMN–25%PT).

Above the Curie temperature of 473 K, the (002) reflection peaks become narrow and shift towards low values. A doublet was observed near 44.9° and 45°, whereas a single is expected in the cubic symmetry. The two peaks were thus related to the cubic phases of two different compositions. The corresponding parameters are equal to 4.018 and 4.026 Å, respectively. The most important peak (4.018 Å) corresponds obviously to the PMN–35%PT since it accounts for approximately ~70% volume of the matrix for sample B. The second one is related to PMN–25%PT cubic templates. It is worth noting that only the {00*l*} reflections are observed for the PMN–25%PT compound since the templates are well oriented along the ⟨001⟩ direction. On the other hand, the peak corresponding to cubic templates which is well observed for sample B, is very weak and observed as a shoulder for sample A with a texture fraction of 0.9.

These results show that for the TCTC disks, the two compounds PMN–25%PT and PMN–35%PT can be distinguished in the cubic phases. For a better estimation of the texture fraction, the Lotgering factor f was then calculated from the XRD spectra recorded at 473° K in the cubic phase.

Table I shows the texture fractions of samples A and B as function of temperature and instruments. The factor f,

Table I. Lotgering factors of textured samples as function of modus operandi, instruments and area fraction by image analysis.

Sample	Cubic phase (473 K)		Ferroelectric phases (295 K)	
XRD instrument	Rotating anode		Seifert	Image Analysis
A	0.99	0.95	0.95	0.95
B	0.90	0.60	0.77	0.35
C	—	—	0.25	0.25
D	—	—	0.15	0.07

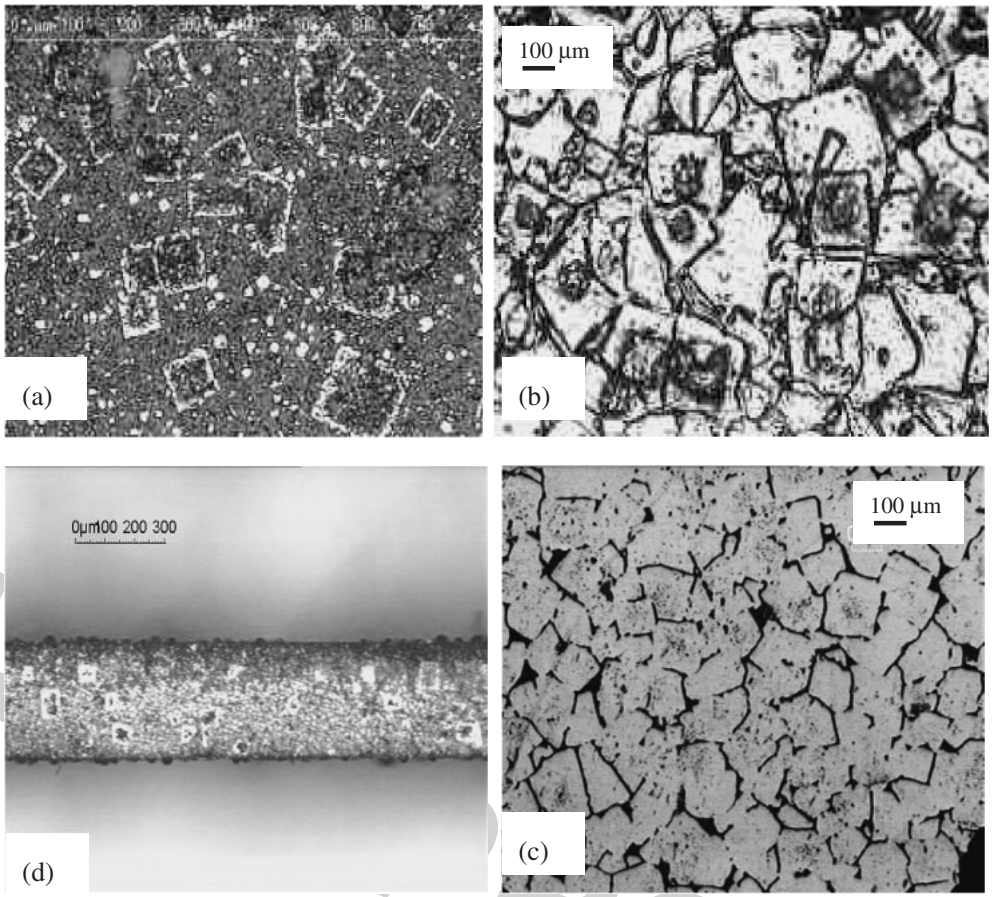

Fig. 3. Optical microphotographs of TCTCs, recorded on as-sintered surface, displaying texture fraction of (a–d) 0.77 and (b–c) 0.9: (a–b) as-sintered surface, (c) lapped and polished surface (150 µm thick were removed from the surface), (d) polished sample cut perpendicular to the disk surface.

determined in the cubic phase, is higher than that calculated using XRD at room temperature. The calculated Lotgering factors are 0.99 and 0.9 in the cubic or paraelectric phase instead of 0.95 and 0.6 in the RT or ferroelectric phase for samples A and B, respectively. For the quasi complete tape cast textured ceramic (sample A), the factors f are 0.95 in the ferroelectric phase, irregardless of the instrument used. For lower texture sample B, the factor f varies slightly from 0.77 to 0.66, depending on the XRD instrument used to record spectra. This is probably due to the optical configuration of each instrument.

3.2 Surface microstructure and fibre texture

Optical microphotographs on as-sintered ceramics show large cubic crystals dispersed inside the ceramic matrix (Fig. 3). In both as-sintered samples, the growth area around the pristine crystal seeds can be clearly observed: crystal cores appear in black and the periphery in white. Sample B presents large cubic grains (about 100 µm) dispersed in the ceramic matrix of small grain size (~3 µm) [Fig. 3(a)]. Sample A exhibits a nearly complete pavement of cubic crystals with residual matrix grains in the crystal boundaries [Fig. 3(b)].

These observations are in accordance with the XRD spectra and confirm that the composition of the grown perovskite can be determined by the matrix composition. The presence of two textured compositions in PMN–PT tape cast textured ceramics, sintered at low temperature, is consistent with ceramic texturing through the liquid phase at the crystal-matrix interface. At high temperature, the matrix is consumed and crystal growth is induced in all the ceramics, under a high PbO partial pressure.

Optical micrographs of as-sintered samples were analysed using an analysis software[15] to characterize the texture morphology. The fraction of oriented material was determined by measuring the area fraction of large cubic grains. Data presented in Table I show that, for the quasi-complete textured sample (A), the area fraction is in accordance with the Lotgering factor determined using XRD. For all other samples, the area fractions are lower than the Lotgering factor. In fact, the microstructure of the textured sample shows that beside large cubic grains, small cubic grains of about 10 µm are observed [Fig. 3(a)]. The difference should be due to the fact that small oriented crystals are not taken into account in the determination of the area fraction.

In order to investigate the orientation relationship between grains, a ω-scan of the {002} peak and (011) pole figure was recorded at RT and on an as-sintered surface. In Fig. 4(a), a ring pattern of the highest contour is observed at $\chi = 44.7^\circ$. This value which corresponds to the angle between (001) and (011) poles (which is equal to 45° for the cubic symmetry), shows that the observed texture is a (001) fibre texture, i.e., with no preferential orientation in the plane. Figure 4(b) shows the ω-scan of the (002) peak with a full width at half maximum (FWHM) of less than 6°. Therefore, the distribution of (00l) direction in textured ceramics is very

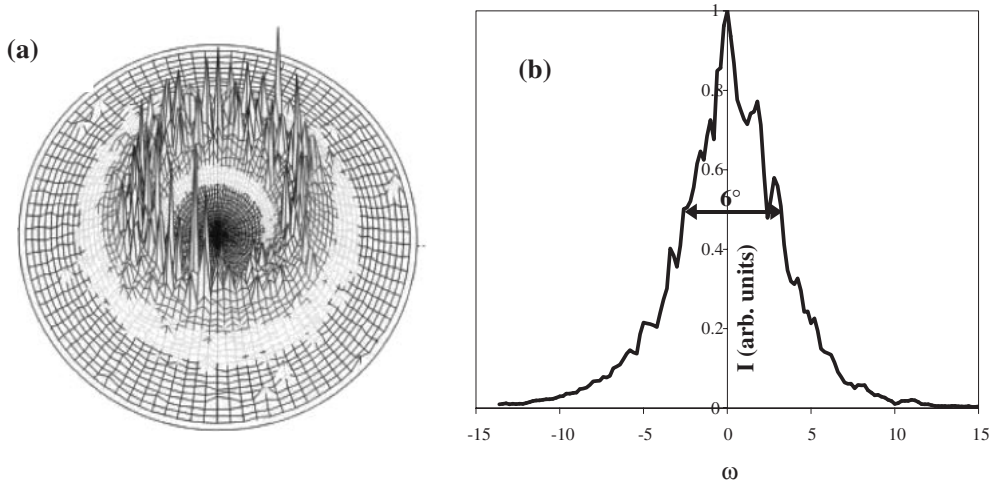

Fig. 4. (a) (011) pole figure of a polished surface of sample B ($f = 0.77$) and (b) ω-scan of the (002) peak, recorded at RT on the as-sintered surface of sample A ($f = 0.95$).

small and out of plan alignment is good.

3.3 Volume texture

Since it is well known that ceramic grain growth kinetics s differ with the surface type and the volume, the texture of the ceramics was determined on a polished surface. An approximately 100 µm thick of ceramic was removed from the as-sintered surface. This thickness represents two individual cast tapes. The polished surface of sample A presents the microstructure of a textured ceramic volume [Fig. 3(c)]. The grains seem to be more homogenous in size than those observed on the as-sintered surface [Fig. 3(b)]. Marks of templates were revealed by the presence of cubic network pores inside the large grains. The marks indicate the random orientation of the grains in the (x, y) plane, as demonstrated above in Fig. 4(a). The Lotgering factor calculated from the XRD spectrum at RT of the polished surface is equal to that obtained from the as-sintered surface ($f = 0.96$). Thus, the orientation of ceramic matrix along the (001) axis was obtained in all volumes considered.

In order to determined the alignment in the thickness direction, sample B was cut perpendicular to the disk surface and polished. Optical micrographs presented in Fig. 3(d) show that the grown large cubic grains were aligned in the thickness direction and the initial green ceramic layers could easily be observed by the superposition of grown cubic grains in the ceramic thickness.

Raman images,[16] mapped on the as-sintered ceramic surface, show that only one PMN–PT composition close to that of the ceramic matrix was observed for sample A while two compositions close to that of the ceramic matrix and the seeds were observed for sample B. Thus, PMN–PT ⟨00l⟩ texturing starts at around 1150°C and increases at a higher temperature. The grown of crystals depends on the neighbouring ceramic matrix, start at around the seeds and is enhanced at the vicinity. Growth rate depends on the sintering temperature and duration. As the crystals grow sufficiently large, they combine into shapes extending from the corners and the edges [Fig. 3(a)]. The observed larger crystals are probably formed by the combination of many small initial seeds [Fig. 3(b)].

3.4 Electromechanical properties

The hysteresis loops obtained with a field amplitude of $15\,\mathrm{kV\cdot cm^{-1}}$ show that the saturated and remanent polarisations of the PMN–PT tape cast textured ceramic (TCTC) are equal to 0.3 and $0.24\,\mathrm{C\cdot m^{-2}}$, respectively, and are close to those of single crystals.[12–15] However, electric coercive fields (E_c) of textured ceramics are close to those of an ceramic. The E_c of (001) textured ceramics are equal to $6\,\mathrm{kV\cdot cm^{-1}}$ while those of (001) oriented single crystals are equal to $2.8\,\mathrm{kV\cdot cm^{-1}}$.[16]

Piezoelectric properties measured at low levels using the IRE method show that the coupling efficiency of the TCTCs ($k_p = 0.66$, $d_{33} = 660\,\mathrm{pC/N}$) is about twice that of TCCs but only 15% better than that of a random optimised disk ceramic. These values are not unfortunately very close to those obtained for (001)-oriented single crystals. This could be due to the lower density measured for textured ceramics (90–95%). TCTC disks with a diameter of 14 mm and a thickness between 0.3 and 1 mm show micro cracks and open pores on the samples. Indeed, at the sintering temperature of TCTC samples, about 1200°C, PbO vapour pressure is very high and some Pb loss is observed despite the use of packaging lead oxide-based powder to control PbO volatilisation.

4. Conclusion

This work demonstrates the feasibility of textured PMN–PT ceramics fabrication by the HTGG technique using PMN–PT cubic templates and nanograins of perovskite powder. A PMN–35%PT ceramic with a quasi complete (001) texture was obtained ($f > 0.95$). Even for this highly textured ceramic, only a fibre texture was obtained. For samples with lower texture fraction, the two compositions evidenced by Raman imaging were consistent with the two textures observed by XRD. The grown perovskite was determined by the matrix composition. Therefore, it is not necessary that the composition of the pristine seed dispersed in the green matrix has the target composition.

It was demonstrated that $(Sr_{0.53},Ba_{0.47})Nb_2O_6$ fibre-textured ceramics[17] exhibit a direct correlation between the degree of fibre texture in the polar direction and the

percentage of single crystal-like properties. As the degree of fibre texture increased in the [001] axis, the piezoelectric coefficient of a high fraction of single crystals increased. In the case of PMN–PT textured ceramics, electromechanical properties at low levels were higher than those of tape cast ceramics, but not significantly higher than those of optimised conventional ceramics. Better performance characteristics were observed at a higher driven electric field ($>5\,kV/cm^2$).[10)]

In this study, a similar behaviour was observed. Regarding the low orientation distribution of highly textured ceramics, we conclude that the poling process and ferroelectric domain reorganisation have to be extensively studied to clarify the behaviour of textured ceramics.

Acknowledgments

This work was supported in part by the "PIRAMID" project under European Fifth Framework Programme.

1) J. Kuwata, K. Uchino and S. Nomura: Jpn. J. Appl. Phys. **21** (1982) 1298.
2) T. R. Shrout, Z. P. Chang, N. Kim and S. Markgraf: Ferr. Lett. **12** (1990) 63.
3) E. Park and T. R. Shrout: J. Appl. Phys. **82** (1997) 1804.
4) R. Zhang, B. Jiang and W. Cao: Appl. Phys. Lett. **82** (2003) 3737.
5) H. Dammak, A. Renault, P. Gaucher, M. Pham Thi and G. Calvarin: Jpn. J. Appl. Phys. **42** (2003).
6) B. Noheda, D. E. Cox, G. Shirane, J. Gao and Z.-G. Ye: Phys. Rev. B **66** (2002) 054104.
7) R. Bertram, G. Reck and R. Uecker: J. Cryst. Growth **253** (2003) 212.
8) A. Kumar Singh and D. Pandey: Phys. Rev. B **67** (2003) 064102.
9) E. M. Sabolsky, A. R. James, S. Kwon, S. Trollier-McKinstry and G. L. Messing: Appl. Phys. Lett. **78** (2001) 2551.
10) E. M. Sabolsky, S. Trollier-McKinstry and G. L. Messing: J. Appl. Phys. **93** (2003) 4072.
11) R. E. Brennan, M. Allahverdi, M. E. Ebrahimi and A. Safari: Proc. 13th IEEE ISAF, 2002, Nara, Japan (2002) p. 435.
12) M. P. Thi, H. Hemery and O. Lacour: US Navy Workshop on Acoustic Transduction Materials & Devices, (2003).
13) J. F. Berar, G. Calvarin and D. Weigel: J. Appl. Crystallogr. **13** (1980) 201.
14) F. K. Lotgering: J. Inorg. Nucl. Chem. **9** (1959) 113.
15) H. Hemery: Thesis, INSA Lyon, 2003.
16) M. P. Thi and Ph. Colomban: to be published in J. European Ceramic Soc.
17) C. Duran, S. Trolier-McKinstry and G. L. Messing: J. Am. Ceram. Soc. **83** (2000) 2203.